

Study of $\text{YBa}_2\text{Cu}_3\text{O}_{7-\delta}/\text{Al}_2\text{O}_3$ Composite for Structural and Electrical transport Property

M.Sahoo, D.Behera

Department of physics, National institute of technology, Rourkela-769008, India

Abstract- The effect of submicron-sized Al_2O_3 particle addition on the crystal structure and superconducting properties of $\text{YBa}_2\text{Cu}_3\text{O}_{7-\delta}$ ceramics was systematically studied. Series of $\text{YBa}_2\text{Cu}_3\text{O}_{7-\delta} + x \text{ Al}_2\text{O}_3$ samples ($x = 0.0, 0.1, 0.2, 0.3, 0.4, 0.5, 0.6$ wt. %) were prepared using the solid state reaction method. The lattice parameters and the orthorhombicity were decreased slightly with Al_2O_3 addition. No change in the structural symmetry state was obtained. SEM micrographs revels the decreasing trend in the grain size of the composite samples. The superconducting transition temperatures (T_c) determined by standard four-probe method was decreased and dropped sharply with higher alumina content. Excess conductivity fluctuation analysis using Aslamazov-Larkin model fitting reveals transition of two dominant regions (2D and 3D) above T_c . The decrease in 2D-3D crossover temperature i.e. Lawerence-Doniach temperature in the mean field region has been observed as a consequent dominance of 3D region to increase in wt. % of Al_2O_3 in the composite.

Index Terms- YBCO, Al_2O_3 , nanoparticle, X-ray diffraction, Electrical properties

I. INTRODUCTION

The high temperature superconductor (HTSC) $\text{YBa}_2\text{Cu}_3\text{O}_{7-\delta}$ (YBCO) is one of the material being considered as potential candidates for applications such as microwave devices, power transmission tape, and delay lines. This is the most useful material for conductor applications because of its high irreversibility field. Superconductivity in YBCO triple perovskite structure resides in the Cu-O planes. It has crystallographically two distinct Cu sites i.e Cu (1) site in CuO chains and Cu (2) in CuO_2 planes. It is known that CuO_2 layers play an important role in transferring of the charge carriers, whereas CuO chains are non-superconducting and acts as ‘charge reservoir’. From the structural point of view, substitution at the Cu (1) site can cause an increase in the oxygen content in the basal plane, inducing orthorhombic to tetragonal (O-T) transition with increasing dopant concentration. If the substitution takes place on Cu (2) site, there is no observed structural O-T transition, the structure remains orthorhombic even for higher dopant concentrations and oxygen order in the CuO chains remains intact [1]. The oxygen in the basal plane acts as a charge reservoir introducing holes into CuO_2 plane copper atoms. The theoretical developments have indicated that the antiferromagnetic spin fluctuations in HTSC favors d-wave pairing. But due to disorder in the structure of the orthorhombic HTSC, distortion of the pairing interaction

takes places, giving rise to s-wave pairing component in the original d-wave pairing. Many experiments have shown that, the CuO_2 sheet in the YBCO structure is a superconducting layer (S) where as the CuO chain layer is a non-superconductor (N) [2]. The hopping interaction between these S-N layers leads to the suppression of T_c [3,4]. Chemical doping in high T_c superconducting cuprates has generated a great interest because it represents an easily controlled, non-destructive and efficient tool for improving the mechanical, structural and superconducting properties of these compounds. Some of the impurities and doping elements suppress superconductivity and may locally modify the crystalline structure and generate defects such as twins, tweed, and inhomogeneous micro-defects, and can act as additional pinning centers, resulting in an increase in the critical current at higher magnetic fields [5-9]. The doping element effects on structural and superconducting properties depend on the dopant material nature and the substitution site. Heterovalent ion substitution in YBCO is of considerable interest, as it can change the lattice constants, the carrier concentration and may influence the charge transfer from the reservoir layers to the conducting layers. The divalent cations substitute at the Cu (2) site but whereas trivalent cations substitute preferentially at the Cu (1) site. The substitution of Cu by non-magnetic ions such as Zn, Al, Ca and Ga or magnetic ions (Cr, Co, Fe) in the high-temperature superconductor is a useful tool for probing superconductivity parameters [10]. XRD analysis reveals that Al substitution does not lead to changes in the structural symmetry of YBCO but decreases the orthorhombicity of the system with an increasing doping level of Al [11]. The value of T_c also decreases with increasing concentration of Al. This indicates that Al exclusively substitutes for the Cu lattice site in YBCO. As Y and Al are isovalent and the ionic radius of Y^{3+} (0.90 \AA°) is higher than the ionic radius of Al^{3+} (0.56 \AA°), there is a good possibility for Al to occupy Y sites when YBCO ceramic is doped with alumina. Thus in this paper we report the results of the structural properties, the electrical resistivity of YBCO ceramics, when Al_2O_3 submicron sized particles are added to them.

II. EXPERIMENTAL PROCEDURE

YBCO powder is prepared by the solid state reaction route by mixing stoichiometric amount of Y_2O_3 , BaCO_3 , CuO followed by grinding, calcination at 880° C , sintering at 920° C and annealing at 500° C for 8 hrs for oxygen uptake respectively. A series of polycrystalline composite samples of (1-x) $\text{YBa}_2\text{Cu}_3\text{O}_{7-\delta} + x \text{ Al}_2\text{O}_3$ ($x=0.0, 0.1, 0.2, 0.3, 0.4, 0.5, 0.6$) were ground and pressed into pellets. The composite pellets were sintered at 920° C for 12

hrs and then cooled to 500°C where they were kept for 5hrs in an oxygen atmosphere for oxygen annealing. XRD was done for phase conformation and structural analysis. SEM was done for microstructural analysis. Temperature dependent resistivity $\rho(T)$ was measured using the standard four-probe techniques with a Nanovoltmeter (Keithley- 2182A) and constant current source (Keithley 6221), with the voltage resolution of 10^{-8} V of the Nanovoltmeter, a constant current source of 1 mA flowing through the samples. A closed cycle helium refrigerator (JANIS) and a temperature controller (Lakeshore 332) having a temperature resolution of ± 0.1 K was used for temperature variation. Computer controlled data-acquisition system was used with a Lab view program.

III. RESULTS AND DISCUSSION

A. XRD analysis

Figure 1 shows the powder X-ray diffraction patterns of the samples of YBCO with Al_2O_3 added and not added. The analysis of the data indicates a predominantly single phase perovskite structure YBCO with orthorhombic P_{mmm} symmetry and small quantities of secondary phases. The lattice parameters were calculated using check cell software. We found that the pure sample has an orthorhombic structure with $a = 3.8175 \text{ \AA}$, $b = 3.8877 \text{ \AA}$, and $c = 11.644 \text{ \AA}$. It should be mentioned that no peaks corresponding to the Al_2O_3 or Al-based compounds were detected by X-ray diffraction. However the EDX result shows that element Al exists in the bulk samples as shown in figure 2 .

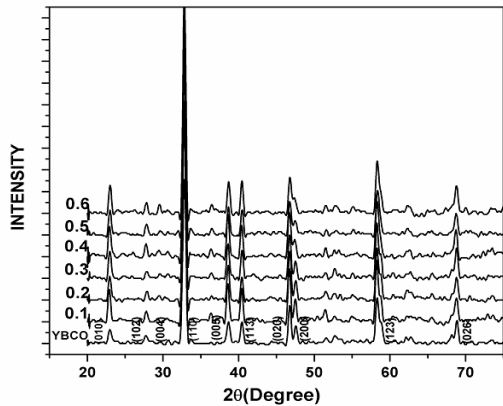


Figure 1: XRD Patterns of $\text{YBCO}+x \text{ Al}_2\text{O}_3$ Samples ($x = 0.0, 0.1, 0.2, 0.3, 0.4, 0.5$ wt. %).

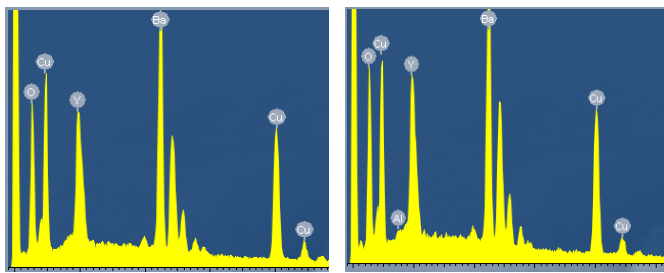


Figure 2: The EDX analysis results taken on the pure YBCO shown in (a) and 0.4 wt.% Al_2O_3 added sample as in (b).

The lattice parameters and unit cell volumes of these samples are presented in table1.

Table I: Parameters calculated from XRD graphs

Al_2O_3 (wt.%)	$a(\text{\AA})$	$b(\text{\AA})$	$c(\text{\AA})$	$V(\text{\AA}^3)$	$\delta=b-a/b+a$	$O_{7-\delta}$
0.0	3.824(3)	3.884(3)	11.641(6)	172.89	0.007	7.0
0.1	3.822(2)	3.880(1)	11.705(4)	173.57	0.007	6.7
0.2	3.819(4)	3.882(2)	11.697(9)	173.41	0.008	6.7
0.3	3.832(2)	3.881(2)	11.675(6)	173.63	0.006	6.8
0.4	3.813(5)	3.882(3)	11.68(2)	172.88	0.008	6.8
0.5	3.844(3)	3.865(2)	11.709(6)	173.96	0.002	6.6
0.6	3.817(8)	3.884(3)	11.684(7)	173.21	0.008	6.8

It may be noticed that the lattice constants ‘a’ and ‘c’ increase with the Al_2O_3 addition while lattice constant ‘b’ remains almost constant as shown from table 1. The addition of Al_2O_3 slightly decreases the difference between a and b parameters and thus reduces the orthorhombicity(δ). The high value of orthorhombicity of the pristine sample is the result of a high oxygen content of the pristine sample with fully occupied O(1) sites in the CuO chains along the b-axis as shown from the $O_{7-\delta}$ value as calculated from the relation $7-\delta = 75.250-5.856c$. With increasing Al_2O_3 content indicates that the orthorhombicity of the system decreases. The slow variation in the a-axis and the changes in the unit cell volume with increasing Al_2O_3 doping level most probably indicate that Al is incorporated into the crystal structure.

B. Microstructural study

The microstructure characterization i.e. grain size distribution of the composites is shown in figure 3. It shows that the pristine YBCO sample exhibits large grains randomly oriented in all directions. The grain size becomes reduced with Al_2O_3 addition. Decrease in grain size indicates that the strength and hardness of the sample increases in Al_2O_3 doped samples.

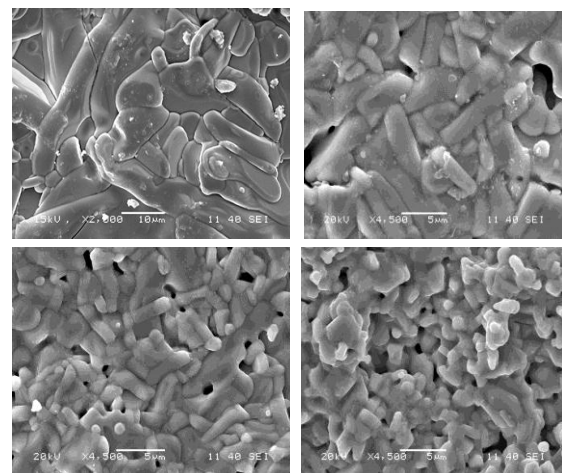


Figure 3: SEM micrographs of $\text{YBCO}+x \text{ Al}_2\text{O}_3$ composites ($x = 0.0, 0.2, 0.4, 0.6$ wt. %) marked as a, b, c, d, respectively

The Al_2O_3 grains contribute in the creation of SNS junctions in the sample microstructure that will improve the current path and thus the conductivity of the samples in the normal state. However in granular HTSCs in the superconducting state(below T_c), transport properties are mainly controlled by the grain boundary microstructure, unlike T_c which is determined by the crystal structure and oxygen content.

C. Temperature derivative of resistivity

Measurements of the resistivity dependence of temperature for different samples with various amounts of Al_2O_3 are shown in figure 4. All samples show metallic behavior in the normal state ($d\rho/dT > 0$) and as superconducting transition to zero resistance. At higher temperature, all samples exhibited linear temperature dependence. The resistive transition exhibits two different regimes. The first is characterized by the normal state that shows a metallic behavior (above $2T_c$). The normal state resistivity is found to be linear from room temperature to a certain temperature, and follows Anderson and Zou relation $\rho_n(T) = A + BT$. Where $\rho_n(T)$ is calculated by using the values of A and B parameters, which are obtained from the linear fitting of resistivity in the temperature range $2T_c$ to 300 K and extrapolated to 0 K gives resistivity slope ($d\rho/dT$) and residual resistivity ρ_0 as seen from figure 4 .

The second is the region characterized by the contribution of Cooper pairs fluctuation to the conductivity below T_c , where $\rho(T)$ is deviating from linearity. This is mainly due to the increasing rate of cooper pair formation on decreasing the temperature. Therefore, the fluctuation induced conductivity in this region follows the AL model to yield the dimensional exponent appropriately to fluctuation-induced conductivity. The normal state resistivity of the composite samples is higher than that of pure sample which is tabulated in table 2. At the temperature value T_{c0} the electrical resistivity vanishes and the phase of the order parameter acquired long range order between the grains of the system. This critical temperature signifies the coherence transition. A finite tailing is observed in the superconducting transition for all the YBCO + x Al_2O_3 composites before the resistance attains zero value. It indicates that the superconducting grains get progressively coupled to each other by Josephson tunneling across the grain boundary weak links. The zero-resistance at the temperature T_{c0} , characterizes the onset of global superconductivity in the samples where the long range superconducting order is achieved. The onset of global resistivity decreases with the addition of Al_2O_3 indicating that it adheres to grain boundary forming weak links . The transition temperature from normal to superconducting state is severely damaged by the addition of Al_2O_3 (shown in table 2) . The depression of T_c with Al_2O_3 addition may be either due to a decrease in oxygen content in the CuO chains [12] or due to trapping of mobile holes or some mechanism connected with the oxygen vacancy disorder . The decrease in T_c by further addition of Al_2O_3 may be caused by over doping of these particles in the YBCO system, and thus a pair-breaking mechanism may occur at a certain doping level. In this regard, small amount of submicron-sized particle addition improved flux pinning by creating effective pinning centers, while excessive Al^{+3} ions doping degraded the superconductivity of the YBCO system. The transition width (ΔT_c) increases with doping concentration. This

may be due to the gradual occurrence of non-superconducting additional phases and the effect of microscopic inhomogeneity.

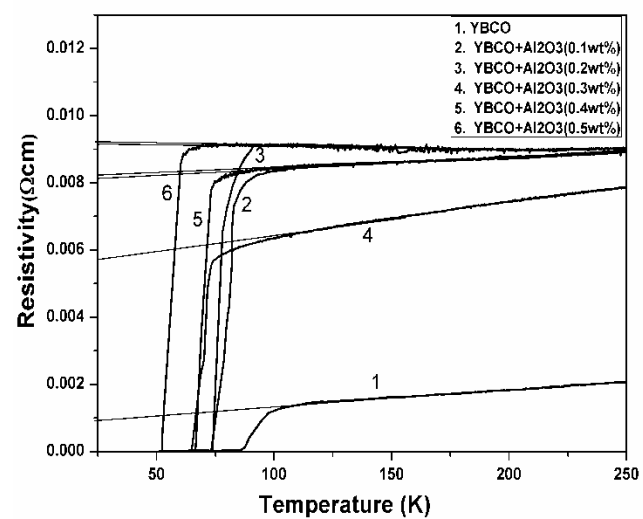


Figure 4: Resistivity dependences on the temperature for YBCO+ x Al_2O_3 ($x=0.0,0.1,0.2,0.3,0.4,0.5$ wt.%) composites.

The percolation factor ‘ α ’ (shown in table 2) arising due to current frustration caused by misalignment of anisotropic grains and sample defects such as voids and cracks are estimated from the temperature coefficient of resistivity $d\rho/dT$.

Table II: Variation of normal state and superconducting parameters in the Composites with different Al_2O_3 wt. %.

Al_2O_3 (wt.%)	T_{c0} (K)	T_c (K)	ΔT_c (K)	α	$\rho_0(\mu\Omega\cdot\text{cm})$
0.0	83.60	89.29	5.69	0.106	892.247
0.1	73.42	81.46	8.04	0.128	7970
0.2	71.33	73.00	1.67	0.511	8820
0.3	64.47	71.40	6.93	0.055	5640
0.4	65.34	66.67	1.33	0.132	8020
0.5	51.57	52.26	0.69	-	9140

This factor contributes to percolate conduction in granular copper oxides. The increasing value of α indicates that the intergranular contribution to the total resistivity decreases. The increasing value of ρ_0 and the decreasing trend in the value of zero-resistance critical temperature (T_{c0}) indicates that the connectivity between grains decreases gradually with the addition of composite . All these effects are due to increased inhomogeneities in the intergranular regions. Point defects and chemical dopants may occupy various positions in a real crystal forming substituent or interstitial impurities. Because of the grain boundary is a structurally distorted region in crystals, an extra energy form in the grain boundary region due to the distortion. As a result of the existence of grain boundary energy as well as the Coulomb interaction between the boundaries and the impurity atoms, they tend to attract impurity atoms in order to decrease the

grain boundary energy. Therefore, the chemical dopant has a higher probability to stay in the grain boundary region than to stay inside the crystal.

D. Excess conductivity

Theoretical Background

The Aslamazov-Larkin (AL) theory provides the following expression for the excess-conductivity above T_c generated by the thermodynamic fluctuations. The fluctuation conductivity $\Delta\sigma$ can be defined as a power-law given by [13]

$$\Delta\sigma = A\varepsilon^\lambda \quad (1)$$

$\Delta\sigma$ is defined by

$$\Delta\sigma = (1/\rho - 1/\rho_R) = \sigma - \sigma_R \quad (2)$$

Where ρ and ρ_R are the measured and normal resistivities, $\sigma(T)$ is the measured conductivity and $\sigma_R(T)$ is the extrapolated conductivity under the assumption of a linear behavior of temperature dependent resistivity. The reduced temperature $\varepsilon = (T-T_c)/T_c$, defined with respect to the mean field critical temperature (T_c) of the normal to superconducting transition. λ is the Gaussian critical exponent depending on the dimensionality of the HTSC system. The dimensionality D of the fluctuation system is related through the expression,

$$\lambda = 2 - D/2. \quad (3)$$

The effective value of the critical exponent for 3D and 2D are $\lambda = -0.5$ and $\lambda = -1$ respectively [14]. A is a temperature dependent parameter and its values for 3D and 2D are $A = e^2/32\hbar\xi(0)$ and $e^2/16\hbar d$ respectively. ' $\xi(0)$ ' is the zero-temperature coherence length or GL correlation length and 'd' is the effective separation of CuO_2 layers. These relations are based on GL theory and are valid only for the mean field temperature region ($1.01T_c$ to $1.1T_c$). Lawrence and Doniach (LD) [15] extended the AL model for layer superconductors, where conduction occurs mainly in 2D CuO_2 planes and these planes are coupled by Josephson tunneling. The excess conductivity parallel to the layers in the LD Model is given by

$$\Delta\sigma(T)_{LD} = e^2/16\hbar d \varepsilon \{1 + (2\xi(0)/d)^2 \varepsilon^{-1}\}^{-1/2} \quad (4)$$

From equation (4) at Temperature close to T_c , $2\xi(0)/d \gg 1$ and $\Delta\sigma(T)$ diverges as $\varepsilon^{-1/2}$ which corresponds to 3D behavior. Where as at $T \gg T_c$, $2\xi(0)/d \ll 1$ and $\Delta\sigma(T)$ diverges as ε^{-1} which corresponds to 2D behaviour.

Figure 5 displays the logarithmic Plot of excess conductivity as a function of reduced temperature (ε). In order to explain the experimental data with theoretical predicted ones, the different regions of the plot were linearly fitted and the exponent values were determined from the slopes. The plot reveals three distinct regimes i.e. mean-field region or the Gaussian fluctuations , critical fluctuations and short wave fluctuation region.

1. Gaussian Fluctuations

In the mean-field region we represent two fits, one with slope value 1.0 and the other with value 0.5. The different

exponents corresponding to crossover temperatures are as follows, the first exponent is in the normal region at $\log \varepsilon (-0.6 \geq \log \varepsilon \geq -1)$ and its values are close to 1, which indicate that the order parameter dimensionalities (OPD) are two dimensional (2D). The second exponent is in the critical field region at $\log \varepsilon (-1 \geq \log \varepsilon \geq -2)$ and its values are close to 0.5, which signifies that the OPD are three dimensional (3D). 3D and 2D behavior of superconducting order parameter fluctuation dominates in YBCO composite. The temperature at which dimensionality fluctuation occurs from 3D to 2D is denoted by Lawrence-Doniach temperature (T_{LD}). T_{LD} values are higher than the T_c values. It reveals that the thermodynamically activated Cooper pairs are generated within the grain at comparatively higher temperatures but due to the intragranular disturbances the mean field critical temperature comes down to lower value. It is possible to infer that this 3D Gaussian regime, determines the spatial limit for the obtainment of long range order of the superconductivity in the material bulk. When the temperature is diminished near T_c , first superconductivity is established in the CuO_2 planes, as a 2D regime, and crosses up to a well defined 3D regime [16].

2. Critical Fluctuations

In superconducting grains Josephson coupling occurs between them. In the absence of magnetic field, their interaction is two dimensional. Considering the Drude like formula for excess conductivity and dynamical scaling theory for coherence length, the critical exponent of excess conductivity is obtained as [17,18]

$$\lambda_{cr} = v (2 - D - \eta + z) \quad (5)$$

Where z is the dynamical exponent, η is the exponent of the order parameter correlation function, D is the dimensionality of the fluctuations and v is the critical exponent for the coherence length. Using this relation for the fluctuation conductivity data in the critical region, one can estimate the dynamical exponent z , [19]. The CuO_2 planes as a common structural element of HTSC's are responsible for their dimensionality and their anisotropic properties [20,21]. According to renormalization group calculations, $v = 0.67$ and $\mu = 0.03$ are expected and $z = 0.32$ being predicted by the theory of dynamical critical scaling [22]. Using these values with $D = 3$ yields $\lambda_{cr} = 0.33$ which is called as the 3D-XY-E because of the model-E dynamics. The critical fluctuation and 3D fluctuation regions intersect at temperature T_G (shown in table 3). Still closer to T_G , a critical scaling regime beyond 3D-XY is observed, labeled by the exponent $\lambda_{cr} = 0.16$ [23,24]. The regime beyond 3D-XY with $\lambda_{cr} = 0.17$ was first observed in the YBCO single crystal . This exponent is known to characterize the critical resistive transition in classical granular arrays formed by metallic superconducting particles embedded in a poorly conducting matrix.

3. Shortwave fluctuations

The excess conductivity varies sharply with exponent value 3 with $\log \varepsilon (-0.5 \geq \log \varepsilon \geq -0.1)$ which highlights the presence of short wave fluctuations. The crossover temperature from 2D to short wave fluctuations (T_{2D-SW}) is indicated in table 3. Short-wavelength fluctuations (SWF) effects appear when the

characteristic wavelength of the order parameter becomes of the order of coherence length [25].

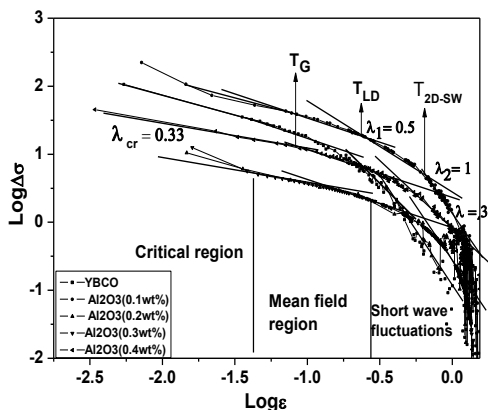


Figure 5: Log-Log plot of excess conductivity $1/\rho - 1/\rho_R$ as a function of reduced Temperature $\epsilon = (T_c - T) / T_c$ in YBCO+ Al_2O_3 composite.

Table III : Al_2O_3 content dependence of different cross over temperatures (Ginzburg-Landau, Lawrence-Doniach and Shortwave fluctuation).

$\text{Al}_2\text{O}_3(\text{wt.\%})$	$T_G(\text{K})$	$T_{LD}(\text{K})$	$T_{SW}(\text{K})$
0.0	96.89	119.02	128.88
0.1	94.17	101.83	122.10
0.2	88.26	93.08	110.99
0.3	72.57	82.49	105.43
0.4	74.93	84.74	110.64
0.5	74.85	83.28	108.48

From the above data it is clear that the different regions observed are the critical region at $T < T_c$, the mean field region at T close to T_c and the short wave fluctuations at $T > T_c$. The different crossover temperatures T_G , T_{LD} , T_{2D-SW} decrease with increase in wt.% .

IV. CONCLUSION

Substitution of aluminum to both copper in chains Cu(1) and yttrium (Y) atoms, does not alter the structural symmetry of $\text{YBa}_2\text{Cu}_3\text{O}_y$ but the orthorhombicity of the system is decreased by increasing the Al_2O_3 content. It may also affect the oxygen content of crystals and the superconducting transition temperature has been shown to be sensitive to the oxygen content. Aslamazov-Larkin (AL) and Lawrence-Doniach (LD) revealed the occurrence of two fluctuation regimes characterized by the critical exponents $\lambda_{3D} = 0.5$ and $\lambda_{2D} = 1.0$ respectively. These regions were interpreted corresponding to 3D and 2D Gaussian regimes respectively, where a crossover from 2D to 3D fluctuations is observed in the mean-field region.

ACKNOWLEDGMENT

The authors gratefully acknowledge the Department of Science and Technology, Govt. of India for providing fellowship to carry out this work.

REFERENCES

- [1] T.A. Mary , U.V. Varadaraju, Structure and superconductivity studies on the Ga doped system, $\text{NdBa}_2\text{Cu}_3-x\text{GaO}_7-\delta$, J Mat. Res. Bull., 1992, pp 447.
- [2] Da-Ning Shi,Zheng-Zhong Li, "The effect of nonmagnetic doping on high-Tc superconductivity", J Physica C,1996, pp 274.
- [3] I.M. Tang, S. Leelaprate, P. Winotai,"Coupling of the orthorhombic distortion to the depression of the Tc's due to N2+doping in the re-123 hsc's:a (d+s) wavepicture", J. Mod. Phys. B, 1999, pp 2291.
- [4] D.A. Wollman , D.J. Van Harlingen, W.C. Lee, D.M.Ginsberg, A.J. Leggett, "Experimental determination of the superconducting pairing state in YBCO from the phase coherence of YBCO-Pb dc SQUIDS", J Phys. Rev. Lett., 1993, pp 2134.
- [5] Y.Zhao, C.H.Cheng, J.S. Wang, " Flux pinning by NiO-induced nano-pinning centres in melt-textured YBCO superconductor",Supercond. Sci. Technol., 2005, pp S43 .
- [6] T.A. Campbell, T.J. Haugan, I. Maartense, J. Murphy, L. Brunke, P.N.Barnes, " Flux pinning effects of Y_2O_3 nanoparticulate dispersions in multilayered YBCO thin films", J Physica C, 2005, pp 423.
- [7] Z.H. He, T. Habisreuther, G. Bruchlos, D. Litzkendorf, W. Gawalek, "Investigation of microstructure of textured YBCO with addition of nanopowder SnO_2 ", J Physica C ,2001,pp 277.
- [8] Z.Q.Yang, X.D. Su, G.W. Qiao, Y.C. Guo, S.X. Dou, F.R.de Boer, "Flux pinning enhancement in Ag-sheathed Bi-2223 tapes by nanometer SiC addition", J Physica C ,1999, pp 136.
- [9] M. Annabi, A.M. Chirgui, F. BenAzzouz, M. Zouaoui, M. Ben Salem, "Addition of nanometer Al_2O_3 during the final processing of (Bi,Pb)-2223 superconductors", J Physica C , 2004, pp 25.
- [10] M. Merz , N. Nucker, P. Schweiss, S. Schuppler, C.T. Chen, V. Chakarian, J. Freeland, Y.U. Idzerda, M. Klaser, G. MullerVogt, T. Wolf , " Site-Specific X-Ray Absorption Spectroscopy of $\text{Y}_{1-x}\text{Ca}_x\text{Ba}_2\text{Cu}_3\text{O}_7-\delta$: Overdoping and Role of Apical Oxygen for High Temperature Superconductivity", J Phys. Rev. Lett., 1998, pp 5192.
- [11] T. Siegrist, L.F. Schneemeyer, J.V. Waszczak, N.P. Singh, , R.L. Opila, B. Batlogg, L.W. Rupp, D.W. Murphy, "Aluminum substitution in $\text{Ba}_2\text{YCu}_3\text{O}_7$ " J Phys. Rev. B ,1987, pp 8365-8368 .
- [12] E. Brecht,W.W. Schmahl, G. Miehe, M. Rodewald,H. Fuess, N.H. Andersen, J. HanbB'mann, T. Wolf, "Thermal treatment of $\text{YBa}_2\text{Cu}_3-x\text{Al}_x\text{O}_6+\delta$ single crystals in different atmospheres and neutron-diffraction study of excess oxygen pinned by the Al substituents", Physica C,1996, pp 53.
- [13] M.Sahoo,B. Bhol,A.Kujur,D.Behera, Dimensionality fluctuation in the superconducting order parameter of $\text{YBa}_2\text{Cu}_3\text{O}_7-\delta+x$ CoFe_2O_4 Composite", AIP Conf. Proc., 2012,pp342.
- [14] X.G. Tang , Q.X. Liu , J. Wang, H.L.W. Chan, "Electric-field dependence of the dielectric properties of sol-gel derived $\text{Ba}(\text{Zr}0.2\text{Ti}0.8)\text{O}_3$ ceramics", J Appl. Phys A, 2009,pp 945.
- [15] J. Lawrence, S. Doniach, " Theory of Layer Structure Superconductors," Proc. 12th Conf. Low-temp. Phys, Kyoto, (Tokyo, Keigaku)1970,pp 361.
- [16] A. Kujur, D. Behera, " DC electrical resistivity and magnetic studies in Yttrium Barium Copper oxide/barium titanate composite thin films", J Thin Solid Films, 2012, pp 2195.
- [17] V.N. Vieira, P. Pureur, J. Schaf, "Effects of Zn and Mg in Cu sites of $\text{YBa}_2\text{Cu}_3\text{O}_7-\delta$ single crystals on the resistive transition, fluctuation conductivity, and magnetic irreversibilities", J Phys. Rev. B, 2002, pp 224506.
- [18] A.Esmaili, H. Sedghi, M. Amniat-Talab, M. Talebian,"Fluctuation-induced conductivity and dimensionality in the new Y-based $\text{Y}_3\text{Ba}_5\text{Cu}_8\text{O}_{18-x}$ superconductor", J Eur.Phys.J.B, 2011,pp 443.
- [19] Y. Zhao, C.H. Cheng , J.S. Wang, " Flux pinning by NiO-induced nano-pinning centers in melt-textured YBCO superconductor", J Supercond. Sci. Technol., 2005, pp S43.

- [20] S.W. Tozer et al, " Measurement of anisotropic resistivity and Hall constant for single-crystal $\text{YBa}_2\text{Cu}_3\text{O}_{7-x}$ ", J Phys. Rev. Lett., 1987, pp 1768.
- [21] T.R. Dinger, T.K. Worthington, W.J. Gollagher, R.L. Sandstorm, " Direct observation of electronic anisotropy in single-crystal $\text{YBa}_2\text{Cu}_3\text{O}_{7-x}$ ", J Phys. Rev. Lett., 1987, pp 2687.
- [22] J.C. Le, J. Guillou Zinn-Justin, " Accurate critical exponents from the $03B5$ -expansion", J Phys. Rev. B., 1980, pp 3976.
- [23] A.R. Jurelo, Jr P. Rodrigues, R.M. Costa, "Analysis of fluctuation conductivity of polycrystalline $\text{Er}_{1-x}\text{Pr}_x\text{Ba}_2\text{Cu}_3\text{O}_{7-\delta}$ superconductors", Brazilian J Physics, 2009, pp 667.
- [24] A. Mohanta, D. Behera, "Fluctuation induced magneto-conductivity studies in $\text{YBa}_2\text{Cu}_3\text{O}_{7-\delta} + x \text{ Ba Zr O}_3$ composite high-T_c superconductors", J Physica C, 2010, pp 295.
- [25] A. Harabor, N.A. Harabor, M. Deletter, "Short-wavelength fluctuation regime in paraconductivity of bulk monophase (Bi, Pb)-2223 superconductor system", J optoelectronics and advanced materials, 2006, pp 1072.

AUTHORS

First Author – Mousumibala Sahoo, Ph.D, NIT, Rourkela
Email: sahoomousumi0@gmail.com

Second Author – Dhrubananda Behera, Ph.D, NIT, Rourkela
Email address: dhrubananda_behera@yahoo.co.in

Correspondence Author – Mousumibala Sahoo,
Email Address: sahoomousumi0@gmail.com, Contact number : 09437864546